

Magnetic-flux tuning of spin chirality in Mott insulators with ring exchanges

Yi-Fei Wang¹ and Chang-De Gong^{1,2}

¹Center for Statistical and Theoretical Condensed Matter Physics, and Department of Physics, Zhejiang Normal University, Jinhua 321004, China

²National Laboratory of Solid State Microstructures and Department of Physics, Nanjing University, Nanjing 210093, China
(Received 2 October 2010; published 27 October 2010)

A peculiar manifestation of the Aharonov-Bohm effect in Mott insulators, presents as a versatile scheme to manipulate the intriguing ground-state spin chirality, such as, tune the magnitude continuously, switch an abrupt jump, or even reverse its sign from a para-chiral phase to a dia-chiral phase. Such an unusual mechanism is due to the coupling between multiple-spin ring exchanges and magnetic flux, and the competition between spin chirality and magnetism, and is demonstrated explicitly in both quasi-one-dimensional ladders and two-dimensional lattices with triangles as elementary plaquettes.

DOI: 10.1103/PhysRevB.82.132406

PACS number(s): 75.10.Jm, 75.50.Ee, 71.10.Hf, 72.80.Sk

I. INTRODUCTION

An elusive but probable noncoplaner spin ordering, spin chirality, has intrigued physicists for decades, and been discussed in various contexts, ranging from spin glass to frustrated quantum magnetism, and from superconductivity to anomalous Hall effect.¹⁻⁵ Of particular interest, the states with spin chirality may have exotic transport^{3,6} and magnetoelectric properties.⁷ For instance, conduction electrons propagating through a chiral spin texture in a frustrated magnet, may experience an effective Berry phase and thus exhibit anomalous Hall effect.³ And if this spin ordering opens a charge excitation gap, even spontaneous quantum-Hall effect will occur.⁶

Given the tremendous interest in spin chirality and its unusual effects, it is desirable to find simple and realistic examples with tunable spin chirality. A possible route is to study Mott insulators (MIs) with multiple-spin ring exchanges (REs) modulated by a magnetic flux. The simplest three-spin RE (3SRE) includes a linear coupling between spin chirality and magnetic flux in MIs.⁷⁻⁹ And a magnetic flux might induce competing Aharonov-Bohm (AB) effects on different RE paths.^{10,11} Such various REs have been found to be essential in solid ³He systems,¹²⁻¹⁵ electron Wigner crystals,^{10,16-18} an organic compound κ -(ET)₂Cu₂(CN)₃,^{8,19} a cuprate La₂CuO₄,^{20,21} and cold atoms in optical lattices.²² Despite these encouraging advances, one still has no quantitative understanding that how can we quantitatively tune the spin chirality and switch it on or off in MIs, it is both of interest and timely to address this problem.

Here we conduct a study of a frustrated quantum spin-1/2 system with 3SRE and four-spin RE (4SRE) modulated by a magnetic flux. Employing exact diagonalization (ED) of finite systems, we consider both a (two-leg) triangular ladder and a two-dimensional (2D) triangular lattice geometry with periodic boundary conditions (PBCs), which are the simplest systems on which both 3SRE and 4SRE are possible. Beyond the weak-magnetic-flux regime, we explore the large parameter space systematically, and demonstrate that: varying the magnetic flux strength with competitive responses of 3SRE and 4SRE interactions, gives a versatile scheme to manipulate the spin chirality in MIs quantitatively, especially

near the phase boundaries of a para-chiral (PC) phase and a dia-chiral (DC) phase.

II. MODEL HAMILTONIAN

With the nearest-neighbor (NN) Heisenberg antiferromagnetic (AFM) coupling, the 3SRE and 4SRE terms modulated by a uniform magnetic flux, the spin-1/2 model Hamiltonian in a triangular ladder/lattice reads

$$H = J \sum_{\langle ij \rangle} \mathbf{S}_i \cdot \mathbf{S}_j - K_3 \sum_{ijk \in \Delta} [e^{i\phi} P_{ijk} + e^{-i\phi} P_{ijk}^{-1}] + K_4 \sum_{ijkl \in \diamond} [e^{i2\phi} P_{ijkl} + e^{-i2\phi} P_{ijkl}^{-1}], \quad (1)$$

where \mathbf{S}_i is the spin operator on site i . P_{ijk} which defined as $P_{123}: |\sigma_1, \sigma_2, \sigma_3\rangle \rightarrow |\sigma_3, \sigma_1, \sigma_2\rangle$, is the cyclic permutation of the three spins sitting on a triangular plaquette, and satisfies $P_{123}^{-1} = P_{123}^\dagger = P_{321}$. And similarly $P_{1234}: |\sigma_1, \sigma_2, \sigma_3, \sigma_4\rangle \rightarrow |\sigma_4, \sigma_1, \sigma_2, \sigma_3\rangle$ for four spins sitting on a rhombus consisting of two elementary triangles. Contrary to ³He systems in which the ³He atoms are neutral, and similar to electron Wigner crystals,^{10,11} a magnetic flux through the exchange path can change the nature of the REs in MIs, owing to the AB effect. ϕ is the magnetic flux threading a triangular plaquette, in units of $\phi_0/2\pi$ ($\phi_0 = hc/e$ is the flux quantum). We focus here on the parameter space with $J, K_3 > 0$ and $K_4 \geq 0$, and vary the ratio J/K_3 and K_4/K_3 with the setting $K_3 = 1$ (as an energy unit).

For our spin-1/2 case, P_{ijk} satisfies $i(P_{123} - P_{321}) = -4\mathbf{S}_1 \cdot \mathbf{S}_2 \times \mathbf{S}_3 \equiv -4\chi_{123}$, where χ_{ijk} represents the local spin chirality.¹ Given a small ϕ , since $e^{i\phi} P_{123} + e^{-i\phi} P_{321} = \cos \phi (P_{123} + P_{321}) - 4 \sin \phi (\mathbf{S}_1 \cdot \mathbf{S}_2 \times \mathbf{S}_3) \approx (P_{123} + P_{321}) - 4\phi \chi_{123}$, the magnetic flux couples linearly to the spin chirality in the low- ϕ limit,⁷⁻⁹ and therefore could probably induce a nonzero chirality density. Here we are concerned with the large parameter space of $\phi \in [0, \pi]$ and hence consider the many-body AB effect induced by a strong magnetic flux.

III. TRIANGULAR LADDERS

We first consider the ladder geometry. We study the ground state (GS) averaged (local) spin chirality

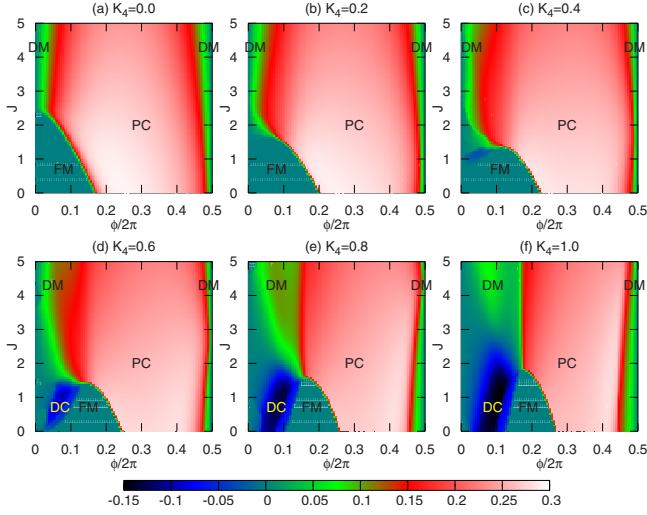


FIG. 1. (Color online) Intensity plots of the GS spin chirality χ_0 in the ϕ - J parameter space (setting $K_3=1$) of the 8×2 triangular ladder at various fixed 4SRE strengths K_4 's. Four typical phases are labeled: FM, dimer (DM), PC, and DC.

$\chi_0 \equiv -\langle \chi_{ijk} \rangle_0$ (here a negative sign is added for convenience) by varying ϕ , J , and K_4 . The typical ED results for a triangular ladder of the size 8×2 are shown in Fig. 1.

In the absence of 4SRE ($K_4=0$), χ_0 is non-negative in the parameter region $\phi \in [0, \pi]$, as shown in Fig. 1(a). Note that χ_0 has the symmetry $\chi_0(\phi) = -\chi_0(-\phi) = -\chi_0(2\pi - \phi)$, which has been numerically confirmed. The whole ϕ - J parameter space is roughly separated into two regions: the bottom left corner ($J \lesssim 2.4$, $\phi/2\pi \lesssim 0.17$, and uniformly colored) with $\chi_0=0$ and saturated ferromagnetic (FM) ($S_{\text{tot}}=S_{\text{max}}$), and larger region with $\chi_0 > 0$ and spin-singlet GSs ($S_{\text{tot}}=0$). We call the $\chi_0 > 0$ state as a PC phase since it can come from the linear coupling between chirality and magnetic flux. The quantum critical line between these two regions has also been verified through tracking the nonanalyticities in the GS energy function $E_0(\phi, J)$.

For the triangular ladders with PBCs, because of the identity $P_{123} + P_{321} = 2S_1 \cdot S_2 + 2S_2 \cdot S_3 + 2S_3 \cdot S_1 + 1/2$, the Hamiltonian with $K_4=0$ will reduce to $H = -N \cos \phi + \tilde{J}_1 \sum_{\langle ij \rangle}^{\text{inter}} \mathbf{S}_i \cdot \mathbf{S}_j + \tilde{J}_2 \sum_{\langle ij \rangle}^{\text{intra}} \mathbf{S}_i \cdot \mathbf{S}_j + 4 \sin \phi \sum_{ijk \in \Delta} \mathbf{S}_i \cdot \mathbf{S}_j \times \mathbf{S}_k$ with $\tilde{J}_1 = J - 4 \cos \phi$ and $\tilde{J}_2 = J - 2 \cos \phi$, where the superscript ‘‘inter’’ (intra) corresponds to the effective interchain (intra-chain) two-spin coupling \tilde{J}_1 (\tilde{J}_2). At the left boundary line of Fig. 1(a) with $\phi=0$, there is a quantum-critical point $J \approx 2.4$ corresponding to $\tilde{J}_2/\tilde{J}_1 = -0.25$ which separates the saturated FM phase²³ and the dimer phase.²⁴ And at the right boundary line of Fig. 1(a) with $\phi=\pi$, the GS is also the dimer phase since $J \geq 0$ and $\phi=\pi$ gives $\tilde{J}_2/\tilde{J}_1 \geq 0.5$.²⁵

In the presence of 4SREs, there are even more interesting behaviors of χ_0 , as shown in Figs. 1(b)–1(f) with five typical K_4 's respectively. At $K_4=0.2$ [Fig. 1(b)], the saturated FM region shrinks in the J direction while expand a little in the ϕ direction. At $K_4=0.4$ and $K_4=0.6$ [Figs. 1(c) and 1(d)], at the center of saturated FM region, there appears a negative- χ_0 region in which the GSs are spin singlets ($S_{\text{tot}}=0$). We call such a negative- χ_0 state as a DC phase, in contrast to the PC

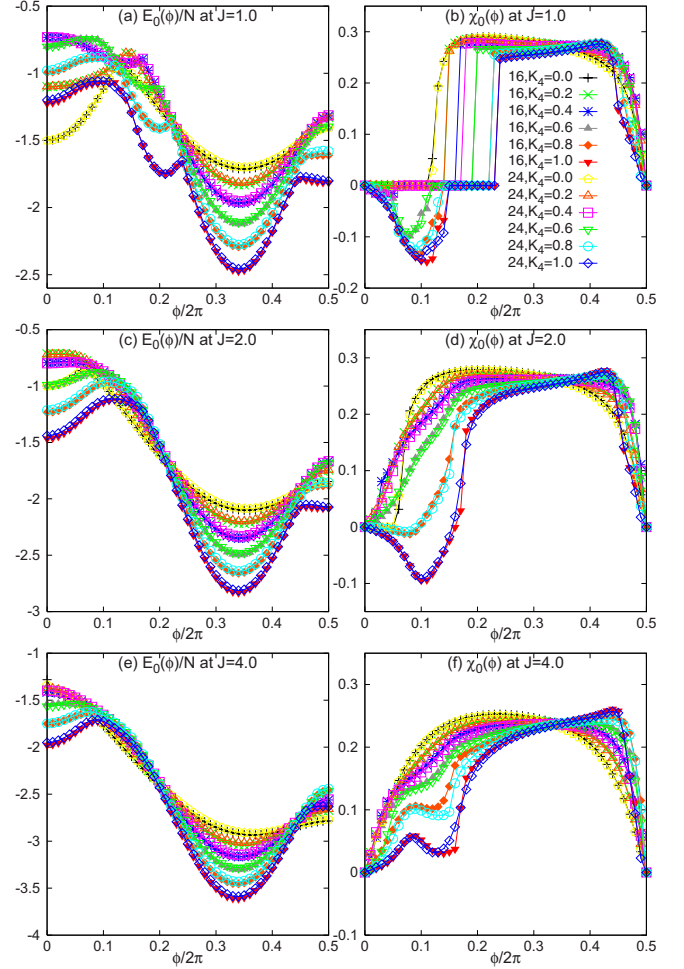


FIG. 2. (Color online) Triangular ladders: GS energy per site E_0/N (left) and GS spin chirality χ_0 (right) versus ϕ , for various J 's, K_4 's, and two ladder sizes N 's.

phase. When K_4 is further increased to 0.8 [Fig. 1(e)] and 1.0 [Fig. 1(f)], the DC region continues to expand and occupies a significant portion in the ϕ - J parameter space.

An intuitive analysis for $K_4 > 0$ is much more difficult, than that in the simpler case of $K_4=0$. However, it should be noted that the 4SRE operators satisfy $P_{1234} - P_{4321} = \frac{1}{2}(P_{123} + P_{234} + P_{341} + P_{412} - \text{H.c.}) = 2i(\chi_{123} + \chi_{234} + \chi_{341} + \chi_{412})$. Therefore, $e^{i2\phi} P_{1234} + e^{-i2\phi} P_{4321} = \cos 2\phi (P_{1234} + P_{4321}) - 2 \sin 2\phi (\chi_{123} + \chi_{234} + \chi_{341} + \chi_{412})$. Due to the opposite signs and the different AB periods of 3SRE and 4SRE terms, the low- ϕ -limit coupling coefficient and the portion of DC region depend on the competitions between them.

In order to address the effects of ladder sizes, we compare two sizes of 8×2 and 12×2 . The mainly considered quantities are χ_0 and the GS energy per site E_0/N . From Figs. 2(a), 2(c), and 2(e), we can see that at the same J and K_4 , the $E_0(\phi)/N$ curves coincide well with each other for both two ladder sizes. And the $\chi_0(\phi)$ curves [Figs. 2(b), 2(d), and 2(f)] also tell that the effects of sizes are already quite small. All these results indicate that in the thermodynamic limit ($N \rightarrow \infty$), at given J and K_4 , both $E_0(\phi)/N$ and $\chi_0(\phi)$ will not deviate obviously from these finite-size results.

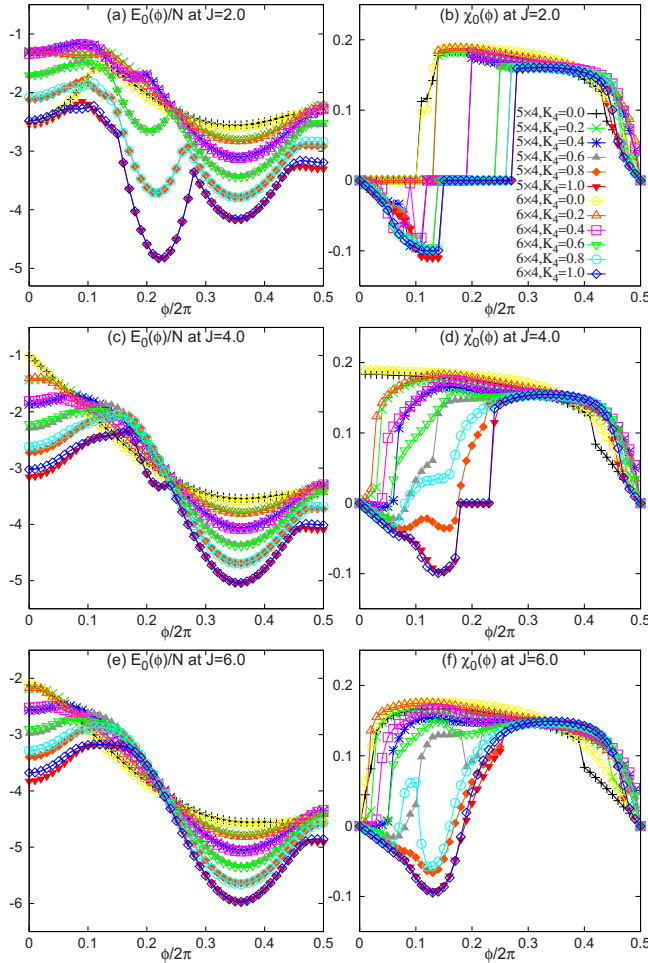


FIG. 3. (Color online) Triangular lattices: E_0/N (left) and χ_0 (right) versus ϕ , for various J 's, K_4 's, and two lattice sizes.

IV. TRIANGULAR LATTICES

For the 2D triangular lattices, we focus on two cases with the sizes of 5×4 and 6×4 (Fig. 3). In the absence of 4SRE terms ($K_4=0$), similar to the previous case of ladders, the Hamiltonian of a 2D triangular lattice with PBCs will reduce to $H = -N \cos \phi + (J-4 \cos \phi) \sum_{\langle ij \rangle} \mathbf{S}_i \cdot \mathbf{S}_j + 4 \sin \phi \sum_{ijk \in \Delta} \mathbf{S}_i \cdot \mathbf{S}_j \times \mathbf{S}_k$. From Fig. 3, we can see that $E_0(\phi)/N$ and $\chi_0(\phi)$ display quite similar behaviors resulting from the competitions between 3SRE and 4SRE terms as the ladders, such as the sign changes and abrupt jumps of χ_0 . We should note that the finite size effects of χ_0 are obvious at some parameter regions; however, the finite size effects of E_0 are always much less significant.

V. LONG-RANGE CORRELATIONS

We now turn to three kinds of correlation functions (CFs) in ladders. The first is the spin-spin CF, defined as $C(r) = \langle \mathbf{S}_i \cdot \mathbf{S}_{i+r} \rangle$, where r is the range (in units of the lattice constant) between two sites along the chain direction and takes integer (half-integer) values for intrachain (interchain) spin-spin CF $C_1(r)[C_2(r)]$. The other two CFs are defined as follows.^{15,19} The dimer operator on a bond (i, j) is defined by

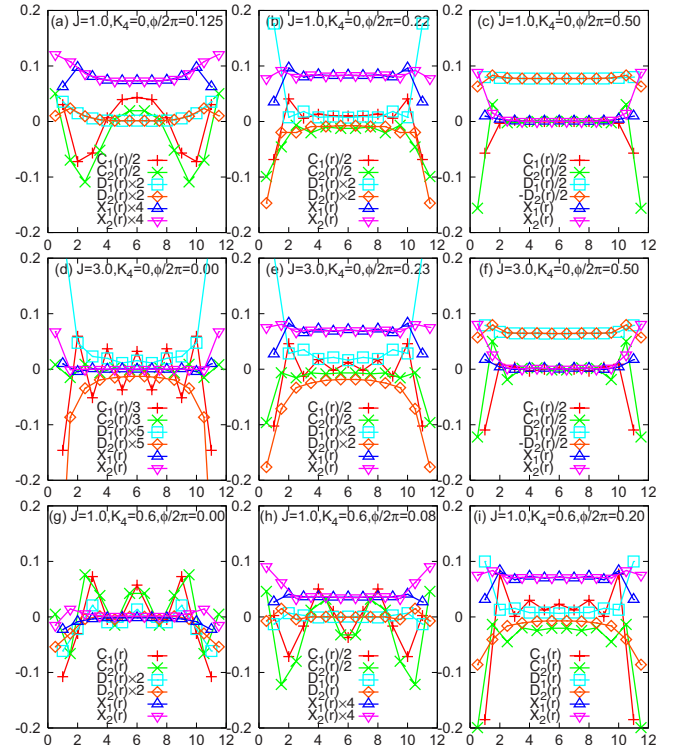


FIG. 4. (Color online) Various GS correlation functions (see text) versus the range r of the 12×2 triangular ladders at various J 's, ϕ 's, and $K_4=0, 0.6$.

$d_{ij} = (1 - P_{ij})/2$ (where $P_{12}: |\sigma_1, \sigma_2\rangle \rightarrow |\sigma_2, \sigma_1\rangle$). The dimer-dimer CF between two bonds is $D(r) = \langle d_{ij} d_{ki} \rangle - \langle d_{ij} \rangle \langle d_{ki} \rangle$ and $D_1(r)[D_2(r)]$ for two parallel (nonparallel) rung bonds between two chains. The chiral-chiral CF between two triangles is defined as $X(r) = \langle \chi_{ijk} \chi_{lmn} \rangle$ and $X_1(r)$ for two up-triangles (or equivalently two down-triangles) while $X_2(r)$ for an up-triangle and a down-triangle.

Now we take the 12×2 triangular ladder as an example and first consider the simpler cases with only 3SREs (Fig. 4 with $K_4=0$). For $J=1.0$, tuning $\phi/2\pi$ across an FM quantum critical point at 0.125 [Fig. 4(a)], both $C_1(r)$ and $C_2(r)$ exhibit that the GS consists of two-period FM domains with opposite magnetization, which is a remnant signature of long-range FM ordering in the FM region; tuning $\phi/2\pi$ further to 0.22 [Fig. 4(b)] at which $\chi_0(\phi)$ takes a maximum, $C_1(r)[C_2(r)]$ shows weak FM (AFM) correlations, and both $X_1(r)$ and $X_2(r)$ reveal nondecaying long-range correlations; when ϕ is increased to π [Fig. 4(c)], $C(r)$'s and $X(r)$'s show fast decaying behaviors, while $D(r)$'s reveal the long-range dimer ordering. For $J=3.0$, $\phi=0$ [Fig. 4(d)], $C_1(r)[C_2(r)]$ shows strong (weak) AFM correlations because of $\tilde{J}_2 > \tilde{J}_1$, and $D(r)$'s also show slowly decaying correlations; tuning $\phi/2\pi$ to make $\chi_0(\phi)$ take a maximum [Fig. 4(e)] and then to 0.5 [Fig. 4(f)], three kinds of CFs resemble the $J=1.0$ cases.

Next, we progress to more interesting cases with 4SREs. For $(J, K_4) = (1.0, 0.6)$, at $\phi=0$ [Fig. 4(g)], the nonzero K_4 makes the long-range FM correlations destroyed, $C(r)$'s and $D(r)$'s exhibit nondecaying fluctuations although $X(r)$'s show fast decaying behaviors; tuning $\phi/2\pi$ to 0.08 [Fig. 4(h)], at which $\chi_0(\phi)$ takes a negative minimum, the $C(r)$'s exhibit

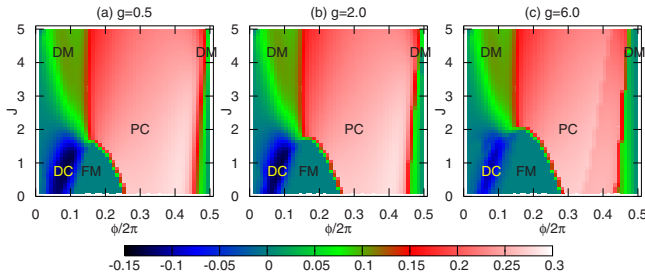


FIG. 5. (Color online) GS spin chirality χ_0 in the ϕ - J parameter space of the 8×2 triangular ladder at $K_4=0.8$ and various effective Zeeman couplings: (a) $g=0.5$; (b) $g=2.0$; and (c) $g=6.0$. Four typical phases are labeled as Fig. 1.

FM domains and $X(r)$'s reveal long-range correlations; then tuning $\phi/2\pi$ to 0.20 [Fig. 4(i)], at which $\chi_0(\phi)$ jumps to a large positive value, $X(r)$'s show long-range correlations.

VI. EFFECTS OF ZEEMAN TERM

In the Hamiltonian model Eq. (1), we have neglected the Zeeman term $H_Z = h_Z S_{\text{tot}}^z = g \phi S_{\text{tot}}^z$. In a real experiment of applying perpendicular magnetic field, the Zeeman term is not negligible. Now we address how our main results might be modified by including a Zeeman term. We take the 8×2 triangular ladder at $K_4=0.8$ as an example, from Figs. 5(a) and 5(b), we can see that a small g does not modify the GS chirality density appreciably; while for a larger g in Fig. 5(c), the DC region shrinks and the FM regions expands, and the overall structure of phase diagram remains almost unchanged. And we can expect an even larger g will align spins

along z direction, thus, in principle, might suppress both DC and PC phases, while favors FM phase.

VII. SUMMARY AND DISCUSSION

For a spin-1/2 system in a triangular ladder/lattice with NN AFM coupling, 3SRE and 4SRE, and a uniform magnetic flux ϕ , we can effectively manipulate the GS spin chirality χ_0 , such as tune continuously the magnitude of χ_0 by varying ϕ , switch an abrupt jump near an FM phase boundary, or even reverse its sign near a transition from a PC to DC phase. The DC phase with negative chirality found here are due to the competition between 3SRE and 4SRE. Various CFs discover the characteristic long-range correlations accompanying the tuned or switched spin chirality.

Such an unusual and versatile manipulation of spin chirality presents a peculiar manifestation of the AB effect on quasilocalized spins in MIs. The experimental observation of these effects is a challenging task, but is probable in 2D organic compound κ -(ET)₂Cu₂(CN)₃, quasi-one-dimensional and 2D Wigner crystals, and cold atoms in optical lattices with REs. For application to Wigner crystals, the phases appearing Eq. (1) are not in general ϕ and 2ϕ , and might be of the order of 2ϕ and 3ϕ for electrons at low densities where 3SRE and 4SRE are comparable.¹⁷

ACKNOWLEDGMENTS

This work was supported by NSFC of China (Grant No. 10904130) and State Key Program for Basic Research of China (Grants No. 2006CB921802 and No. 2009CB929504). ED calculations were based on TITPACK Ver. 2 package by H. Nishimori.

- ¹X. G. Wen, F. Wilczek, and A. Zee, *Phys. Rev. B* **39**, 11413 (1989).
- ²H. Kawamura, *Phys. Rev. Lett.* **68**, 3785 (1992).
- ³Y. Taguchi, Y. Ohawa, H. Yoshizawa, N. Nagaosa, and Y. Tokura, *Science* **291**, 2573 (2001).
- ⁴D. Grohol, K. Matan, J. H. Cho, S. H. Lee, J. W. Lynn, D. G. Nocera, and Y. S. Lee, *Nature Mater.* **4**, 323 (2005).
- ⁵H. Yao and S. A. Kivelson, *Phys. Rev. Lett.* **99**, 247203 (2007).
- ⁶I. Martin and C. D. Batista, *Phys. Rev. Lett.* **101**, 156402 (2008).
- ⁷L. N. Bulaevskii, C. D. Batista, M. V. Mostovoy, and D. I. Khomskii, *Phys. Rev. B* **78**, 024402 (2008).
- ⁸O. I. Motrunich, *Phys. Rev. B* **72**, 045105 (2005); **73**, 155115 (2006).
- ⁹D. S. Rokhsar, *Phys. Rev. Lett.* **65**, 1506 (1990); D. Sen and R. Chitra, *Phys. Rev. B* **51**, 1922 (1995).
- ¹⁰T. Okamoto and S. Kawaji, *Phys. Rev. B* **57**, 9097 (1998); T. Okamoto, K. Hosoya, S. Kawaji, and A. Yagi, *Phys. Rev. Lett.* **82**, 3875 (1999).
- ¹¹B. Bernu, P. Gianinetti, L. Cândido, and D. M. Ceperley, *Int. J. Mod. Phys. B* **17**, 4965 (2003).
- ¹²D. J. Thouless, *Proc. Phys. Soc. London* **86**, 893 (1965).
- ¹³M. Roger, J. M. Delrieu, and J. H. Hetherington, *Rev. Mod. Phys.* **55**, 1 (1983).
- ¹⁴T. Momoi, K. Kubo, and K. Niki, *Phys. Rev. Lett.* **79**, 2081 (1997); K. Kubo and T. Momoi, *Z. Phys. B* **103**, 485 (1997).

- ¹⁵G. Misguich, B. Bernu, C. Lhuillier, and C. Waldtmann, *Phys. Rev. Lett.* **81**, 1098 (1998); G. Misguich, C. Lhuillier, B. Bernu, and C. Waldtmann, *Phys. Rev. B* **60**, 1064 (1999).
- ¹⁶M. Roger, *Phys. Rev. B* **30**, 6432 (1984).
- ¹⁷B. Bernu, L. Cândido, and D. M. Ceperley, *Phys. Rev. Lett.* **86**, 870 (2001).
- ¹⁸A. D. Klironomos, J. S. Meyer, T. Hikihara, and K. A. Matveev, *Phys. Rev. B* **76**, 075302 (2007).
- ¹⁹D. N. Sheng, O. I. Motrunich, S. Trebst, E. Gull, and M. P. A. Fisher, *Phys. Rev. B* **78**, 054520 (2008); D. N. Sheng, O. I. Motrunich, and M. P. A. Fisher, *ibid.* **79**, 205112 (2009).
- ²⁰R. Coldea, S. M. Hayden, G. Aeppli, T. G. Perring, C. D. Frost, T. E. Mason, S.-W. Cheong, and Z. Fisk, *Phys. Rev. Lett.* **86**, 5377 (2001).
- ²¹A. M. Toader, J. P. Goff, M. Roger, N. Shannon, J. R. Stewart, and M. Enderle, *Phys. Rev. Lett.* **94**, 197202 (2005).
- ²²H. P. Büchler, M. Hermele, S. D. Huber, M. P. A. Fisher, and P. Zoller, *Phys. Rev. Lett.* **95**, 040402 (2005).
- ²³T. Hamada, J. Kane, S. Nakagawa, and Y. Natsume, *J. Phys. Soc. Jpn.* **57**, 1891 (1988).
- ²⁴C. K. Majumdar and D. K. Ghosh, *J. Math. Phys.* **10**, 1388 (1969); **10**, 1399 (1969).
- ²⁵T. Tonegawa and I. Harada, *J. Phys. Soc. Jpn.* **56**, 2153 (1987); K. Okamoto and K. Nomura, *Phys. Lett. A* **169**, 433 (1992).